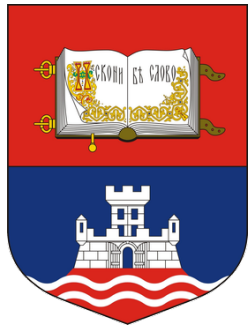

УНИВЕРЗИТЕТ У БЕОГРАДУ
ИНСТИТУТ ЗА ФИЗИКУ | БЕОГРАД
ИНСТИТУТ ОД НАЦИОНАЛНОГ ЗНАЧАЈА ЗА РЕПУБЛИКУ СРБИЈУ

Exploring different high-$p_\perp$ parton energy loss scenarios in pre-equilibrium QCD matter

Bojana Ilic (Blagojevic)

Institute of Physics Belgrade

University of Belgrade

The pre-equilibrium stage of quark-gluon plasma

- The dynamics of early evolution and hydrodynamization of QGP - one of the major sources of uncertainty in HIC studies
- Traditionally, **low-$p_\perp$ sector** ($p_\perp \leq 5$ GeV) is used to study bulk medium properties and the pre-equilibrium stages of the QGP

F. Gelis and B. Schenke, ARNPS 66, 73 (2016);

P. Romatschke EPJC 75, 305 (2015);

G. Aad et al.,JHEP 1311, 183 (2013)

H. Niemi, G. S. Denicol, H. Holopainen and

P. Huovinen, PRC 87, 054901 (2013)

Kurkela, A. Mazeliauskas, J. F. Paquet, S. Schlichting

and D. Teaney, PRL 122, 122302 (2019)

Y. Akamatsu, Nucl. Phys. A 1005, 122000 (2021)

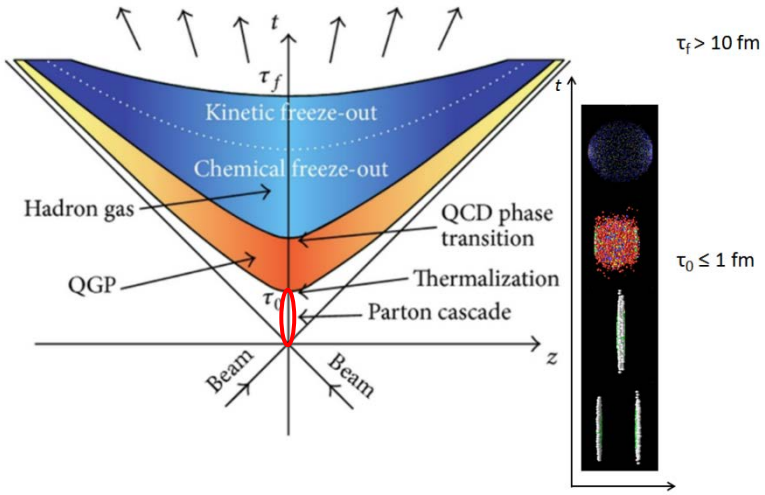

- Commonly, rare **high-$p_\perp$ probes** ($p_\perp \geq 5$ GeV) are utilized for studying the nature of jet-medium interaction

High-$p_\perp$ observables as a novel tool for PE studies

- **High $p_\perp$ partons effectively probe** QGP properties, which in turn depend on early QGP states.
- A **wealth of high-$p_\perp$ experimental data** is available.

JHEP 1811, 013; JHEP 1704, 039; ATLAS-CONF-2017-012; JHEP 1807, 103; PLB 776, 195; EPJC 78, 997.

IJMPCS 46, 1860018; NPPP 289–290, 249; PRL 120, 102301; PRL 120, 202301.

NPPP 289–290, 229.

- However, to our knowledge, a model that quantitatively describes interactions of high-$p_\perp$ particles with the medium in the **pre-equilibrium stage** still does not exit.

Our idea: qualitatively explore the strength of interactions in pre-equilibrium stage:

With this goal:

✓Use our Dynamical energy loss formalism:

- State-of-the-art energy loss in post-equilibrium, i.e., QGP phase.
- Does not use fitting parameters, so it allows using ***both*** high-$p_\perp$ R_{AA} and v_2 data to constrain the bulk properties.
- Temperature profile is the only (intrinsic) input/parameter.

✓Assume that this formalism is applicable to pre-equilibrium stage as well, though we modulate **the strength of interactions** by assuming **different temperature profiles**.

The dynamical energy loss formalism

✓ **Includes:**

- *Finite size finite temperature* QCD medium of *dynamical* (moving) partons
- Based on finite T field theory and generalized HTL approach

M. Djordjevic, PRC 74, 064907 (2006); PRC 80, 064909 (2009), M. Djordjevic, U. Heinz, PRL 101, 022302 (2008)

- Same theoretical framework for both radiative and collisional energy loss
- Applicable to both light and heavy flavor
- Finite magnetic mass effects M. Djordjevic and M. Djordjevic, PLB 709, 229 (2012)
- Running coupling M. Djordjevic and M. Djordjevic, PLB 734, 286 (2014)
- Relaxed soft-gluon approximation B. Blagojevic, M. Djordjevic, M. Djordjevic, PRC 99, 024901, (2019)

All ingredients necessary to accurately reproduce high-$p_\perp$ R_{AA} data!

B.Blagojevic and M. Djordjevic
JPG 42, 075105 (2015)
(highlighted in LabTalk)

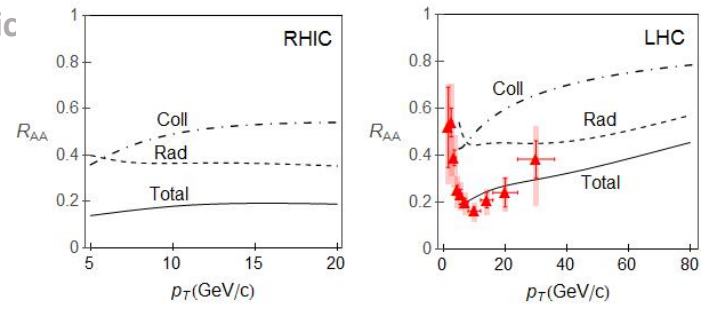

Integrated in DREENA (Dynamical Radiative and Elastic ENergy loss Approach) framework to provide predictions for high-$p_\perp$ observables.

DREENA-B predictions (1D Bjorken expansion)

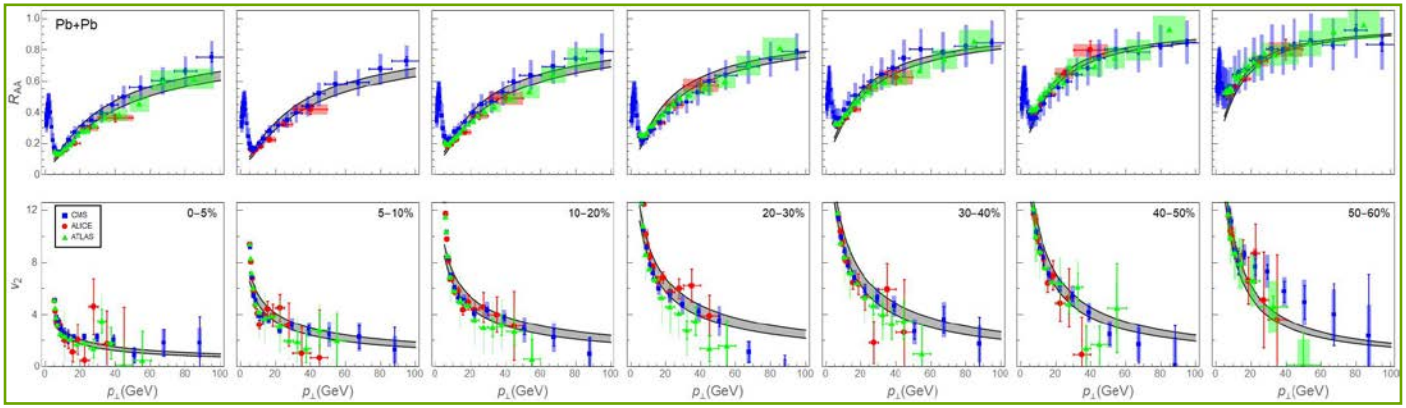

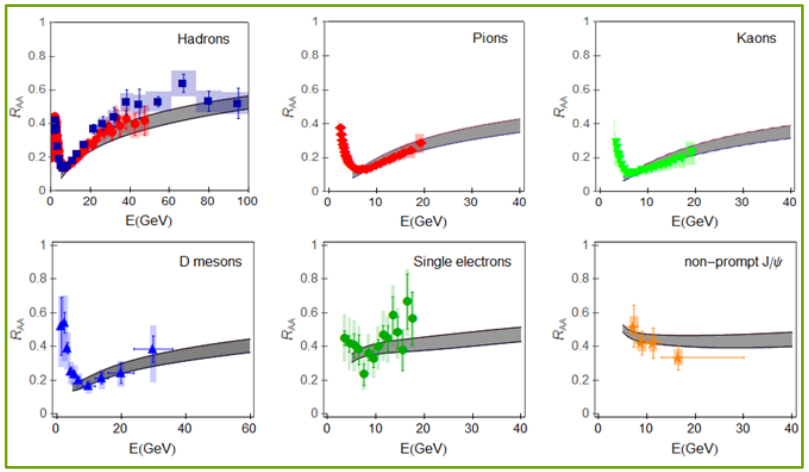

D. Zigic, I. Salom, M. Djordjevic and M. Djordjevic, PLB 791, 236 (2019)

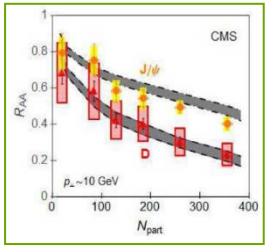

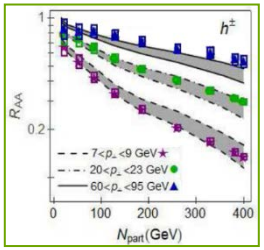

Explains high-$p_\perp$ data for different probes, collision energies, and centralities.

DREENA-B is the framework that we will use in our further analysis.

Why DREENA-B?

The full-fledged DREENA-B (Dynamical Radiative and Elastic ENergy loss Approach + Bjorken expansion) framework, because:

D. Zigic, I. Salom, M. Djordjevic and M. Djordjevic, PLB 791, 236 (2019)

- ✓Dynamical energy loss formalism:
  - T is intrinsic input M. Djordjevic and M. Djordjevic, PLB 734, 286 (2014)
- ✓Bjorken 1D: J. D. Bjorken, PRD 27, 140 (1983)
  - Is analytically tractable
  - Allows analytical introduction of different T-profiles before, and the same upon hydrodynamization
  - Is highly suitable for analytically exploring **different pre-equilibrium energy loss scenarios**

Therefore, DREENA-B provides an optimal framework for early evolution study, as it combines state-of-the-art energy loss model with fully controlled temperature profiles.

Four simple pre-equilibrium T profiles

J. Xu, A. Buzzatti and M. Gyulassy, JHEP 1408, 063 (2014)

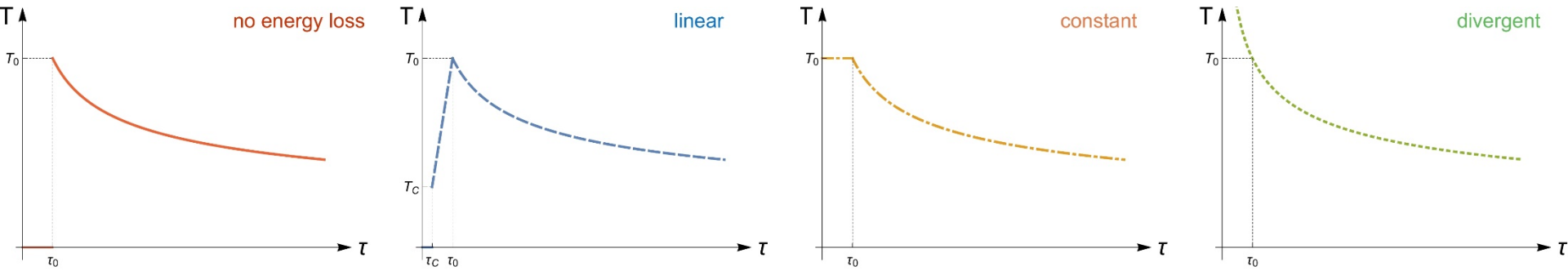

✓The same 1D Bjorken T profile after hydrodynamization, but differ for $\tau < \tau_0$=0.6 fm: PRD 90,094503 (2014)

a) ***No energy loss*** *(T=0)* in pre-equilibrium stage

b) ***Linear***, linearly increasing *T* from T_C=*160 MeV* to T_0=*391 MeV*

(*30-40% 5.02 TeV Pb+Pb*)

c) ***Constant***, $T=T_0$

d) ***Divergent***, Bjorken expansion from the beginning *(τ = 0)* →

the largest energy loss in pre-equilibrium stage

D. Zigic, B. Ilic, M. Djordjevic and M. Djordjevic, Phys. Rev. C 101, 064909 (2020)

Sensitivity of high-$p_\perp$ R_{AA} to PE energy loss scenarios

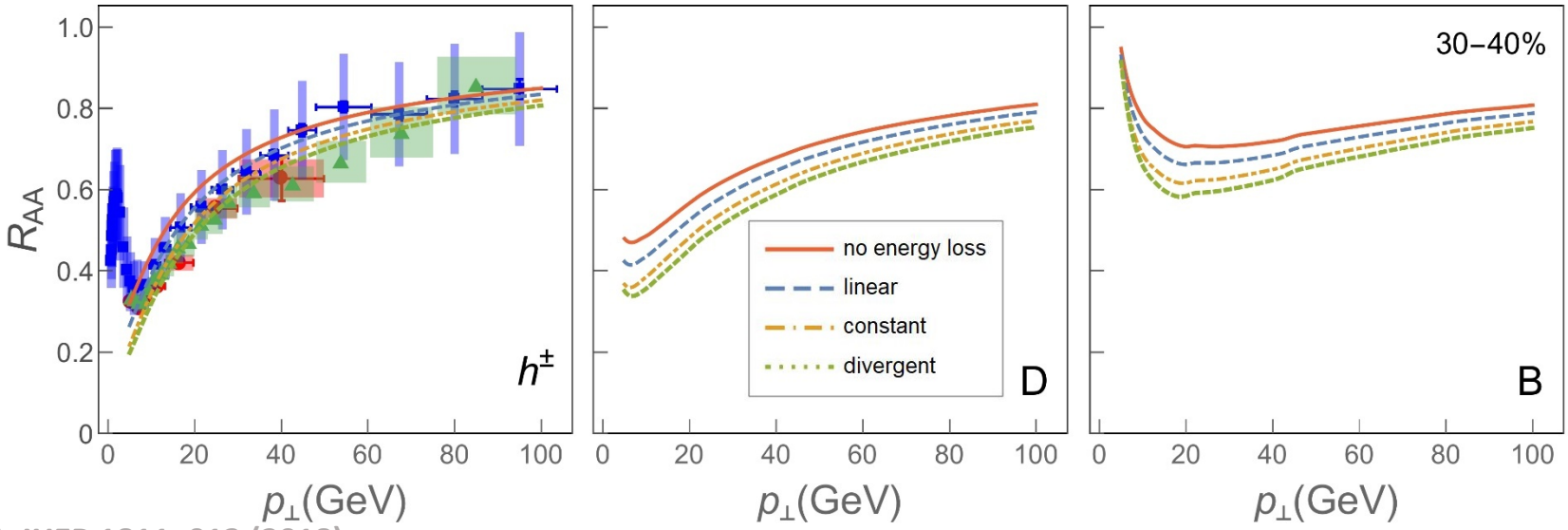

ALICE: JHEP 1811, 013 (2018);
ATLAS-CONF-2017-012;
CMS: JHEP 1704, 039 (2017).

High-$p_\perp$ R_{AA} is notably affected by the presumed PE energy loss scenarios, due to difference in energy loss.

However, higher-precision measurements are required to allow distinguishing between these different scenarios.

D. Zigic, B. Ilic, M. Djordjevic and M. Djordjevic, Phys. Rev. C 101, 064909 (2020)

Explanation of R_{AA} results through analytical estimate

- ✓ R_{AA} is shown to be sensitive only to the averaged properties of the evolving medium

$$1 - R_{AA} \sim \frac{\Delta E}{E} \sim \overline{T}^{a} \qquad a \approx 1.2$$

S. Stojku, B. Ilic, M. Djordjevic and M. Djordjevic, PRC 103, 024908 (2021)

Analytical estimate, but for all predictions we apply full-fledged numerical calculations!

D. Zigic, I. Salom, M. Djordjevic and M. Djordjevic, PLB 791, 236 (2019)

T. Renk, PRC 85, 044903 (2012)

D. Molnar and D. Sun, NPA 932, 140 (2014); 910-911, 486 (2013)

Different $\overline{T}$s for four PE scenarios result in different R_{AA}s.

D. Zigic, B. Ilic, M. Djordjevic and M. Djordjevic, Phys. Rev. C 101, 064909 (2020)

Sensitivity of high-$p_\perp$ v_2 to PE energy loss scenarios

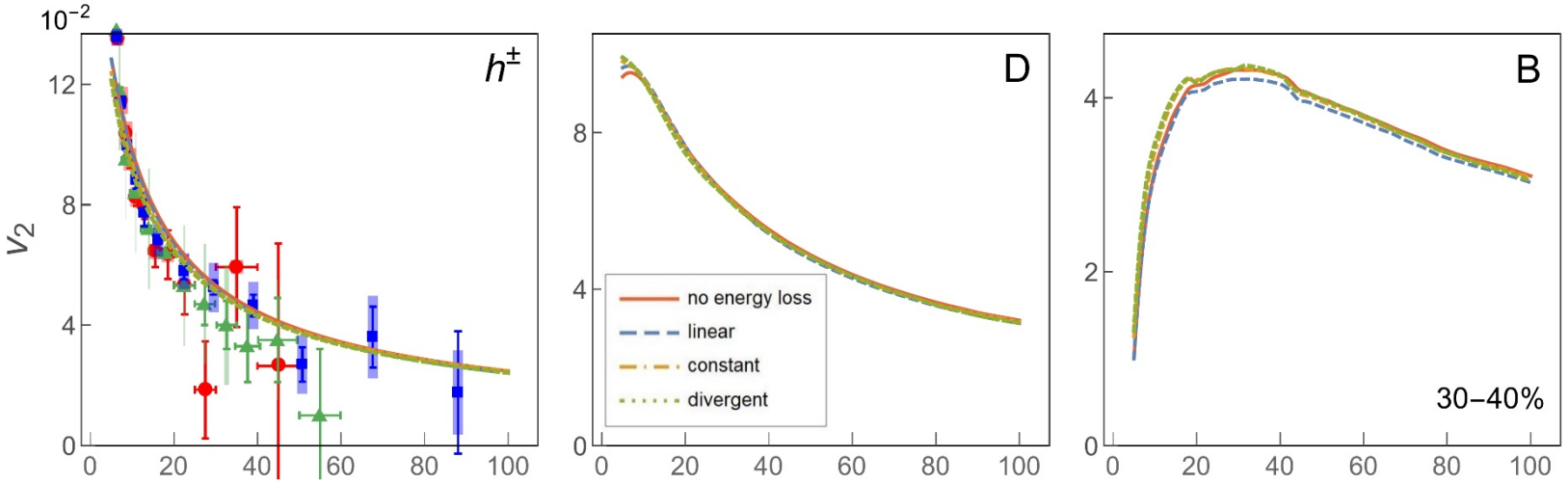

ALICE: JHEP 1807, 103 (2018);
ATLAS: EPJC 78, 997 (2018);
CMS: PLB 776, 195 (2018).

v_2 is insensitive to the pre-equilibrium stages!

C. Andres, N. Armesto, H. Niemi, R. Paatelainen, C. A. Salgado, PLB 803, 135318 (2020)

High-$p_\perp$ v_2 is unable to differentiate between different early time evolution scenarios!

D. Zigic, B. Ilic, M. Djordjevic and M. Djordjevic, Phys. Rev. C 101, 064909 (2020)

Quantitative explanation of the obtained results

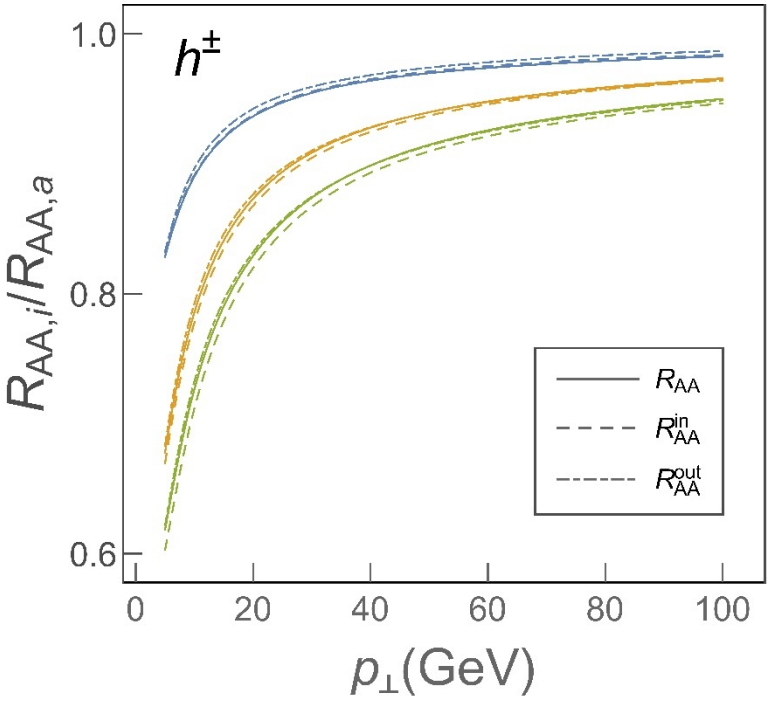

$$R_{AA} \approx \frac{R_{AA}^{in} + R_{AA}^{out}}{2} \qquad v_2 \approx \frac{1}{2}\frac{R_{AA}^{in} - R_{AA}^{out}}{R_{AA}^{in} + R_{AA}^{out}}$$

JHEP 1408, 063

- *Blue* = *Linear*/*No energy loss*
- Orange = *Constant*/*No energy loss*
- Green = *Divergent*/*No energy loss*

Sets of curves

Proportionality functions: $i = lin, const, div$

$$\gamma_i = \frac{R_{AA,i}}{R_{AA,nel}} \qquad \gamma_i^{in} = \frac{R_{AA,i}^{in}}{R_{AA,nel}^{in}} \qquad \gamma_i^{out} = \frac{R_{AA,i}^{out}}{R_{AA,nel}^{out}}$$

$$\gamma_i^{in} \approx \gamma_i^{out} \approx \gamma_i$$

$$\forall i \in \{Blue, Orange, Green\}$$

$$R_{AA,i} \approx \frac{\gamma_i (R_{AA,nel}^{in} + R_{AA,nel}^{out})}{2} = \gamma_i R_{AA,nel} \qquad \gamma_i < 1$$

$$v_{2,i} \approx \frac{1}{2}\frac{\gamma_i (R_{AA,nel}^{in} - R_{AA,nel}^{out})}{\gamma_i (R_{AA,nel}^{in} + R_{AA,nel}^{out})} = v_{2,nel}$$

D. Zigic, B. Ilic, M. Djordjevic and M. Djordjevic, Phys. Rev. C 101, 064909 (2020)

What about a sophisticated hydrodynamical model?

S. Stojku, J. Auvinen, M. Djordjevic, P. Huovinen and M. Djordjevic, arXiv: 2008.08987

Divergent is disfavored.

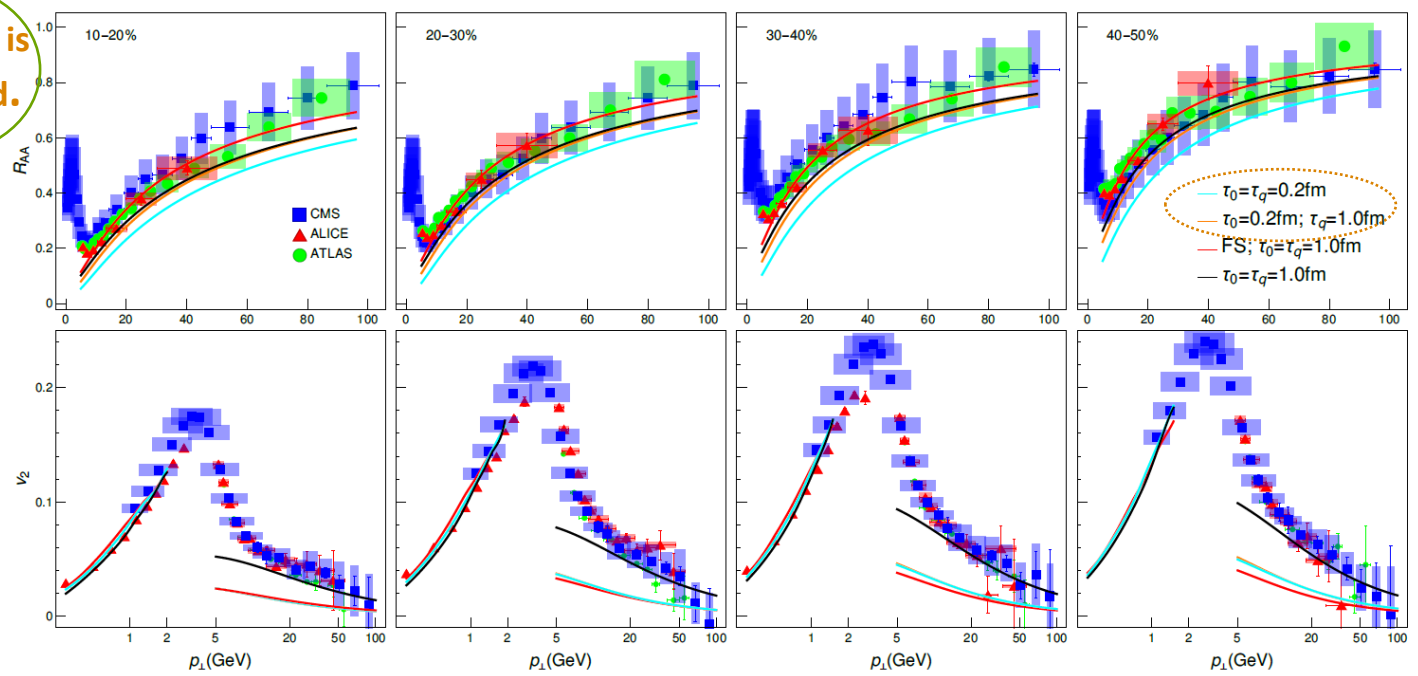

DREENA-A

Cyan ~ *divergent*
Orange ~ *no E-loss*

E. Molnar, H. Holopainen, P. Huovinen and H. Niemi, PRC 90, 044904 (2014)

Even when a sophisticated bulk evolution model is employed, R_{AA} and not v_2 displays sensitivity to the pre-equilibrium energy loss!

Conclusions

- **The pre-equilibrium dynamics of QGP evolution is still an ongoing challenge, with major insight provided by low-$p_\perp$ sector.**
- **We proposed to utilize high-$p_\perp$ particles energy loss, as a complementary tool, to elucidate these early stages of QGP evolution.**
- **We employed our state-of-the-art dynamical energy loss formalism embedded in simple 1D Bjorken medium expansion: DREENA-B framework, to test four straightforward distinct scenarios, ranging from none to very large energy loss in pre-equilibrium stage.**
- **Thus obtained high-$p_\perp$ R_{AA} and v_2 predictions for $h^\pm$, D and B mesons are compared with 5.02 TeV LHC data.**
- **Contrary to common expectations, we obtained that high-$p_\perp$ v_2 is unable to distinguish between different scenarios, being insensitive to the pre-equilibrium stages of medium evolution.**
- **High-$p_\perp$ R_{AA} is sensitive to these diverse cases, and could provide an insight in the early stages' dynamics.**
- **However, higher-precision measurements of high-$p_\perp$ R_{AA} are required to allow for more reliable conclusions through this observable.**

European Research Council

Established by the European Commission

МИНИСТАРСТВО ПРОСВЕТЕ,
НАУКЕ И ТЕХНОЛОШКОГ РАЗВОЈА

In collaboration with: Magdalena Djordjevic, Marko Djordjevic, Pasi Huovinen, Jussi Auvinen, Igor Salom, Dusan Zigic and Stefan Stojku

Thank you for your attention!

Backup

Computational scheme for jet suppression

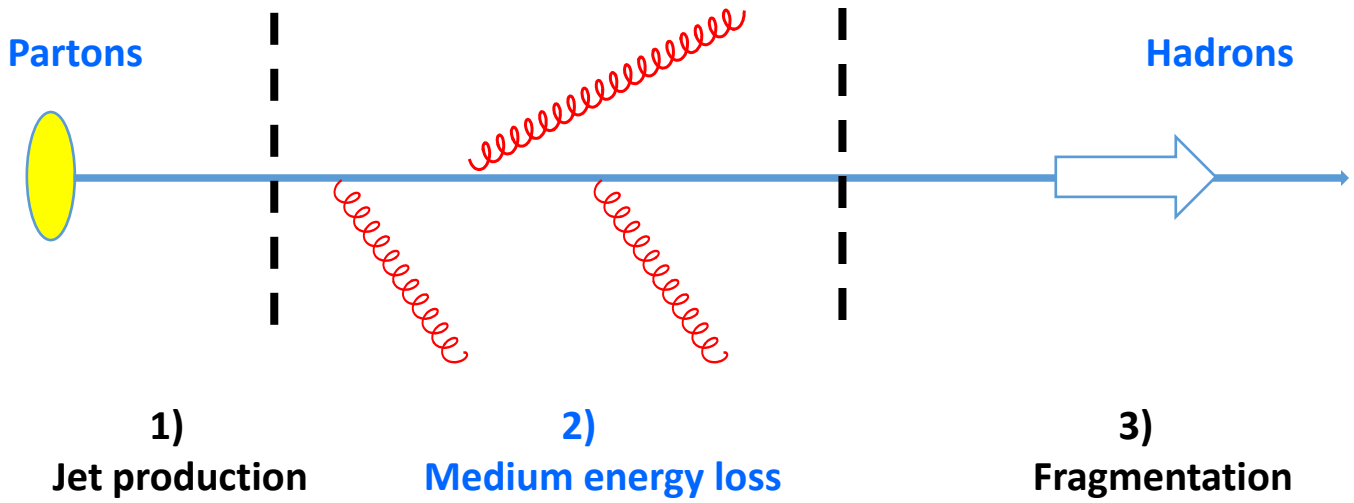

1) **Initial momentum distributions**
2) **Energy loss calculation**
3) **Fragmentation function**

Computational framework

$$\frac{E_f d^3\sigma}{dp_f^3} = \frac{E_i d^3\sigma(Q)}{dp_i^3} \otimes P(E_i \to E_f) \otimes D(Q \to H_Q)$$

- **Light and heavy flavor production**
  Z.B. Kang, I. Vitev, H. Xing, PLB 718:482 (2012); R. Sharma, I. Vitev, and B. W. Zhang, PRC 80, 054902 (2009)
- **Dynamical energy loss in a finite size QCD medium**
  M. Djordjevic and M. Djordjevic, PLB 734, 286 (2014)
- **Multi-gluon fluctuations**
  M. Gyulassy, P. Levai, I. Vitev, PLB 538,282 (2002)
- **Path-length fluctuations**
  A. Dainese, EPJ C33:495 (2004); S. Wicks, W. Horowitz, M. Djordjevic and M. Gyulassy, NPA 784, 426 (2007); D. Zigic, I. Salom, J. Auvinen, M. Djordjevic and M. Djordjevic, JPG 46, 085101 (2019)
- **Fragmentation for light and heavy flavor**
  DSS: D. de Florian, R. Sassot, M. Stratmann, PRD 75:114010 (2007);
  BCFY: E. Braaten, K.-M. Cheung, S. Fleming, and T. C. Yuan, PRD 51, 4819 (1995); M. Cacciari, P. Nason, JHEP 0309: 006 (2003)
  KLP: V. G. Kartvelishvili, A. K. Likhoded, and V. A. Petrov, PLB 78, 615 (1978)

Modified temperature profiles

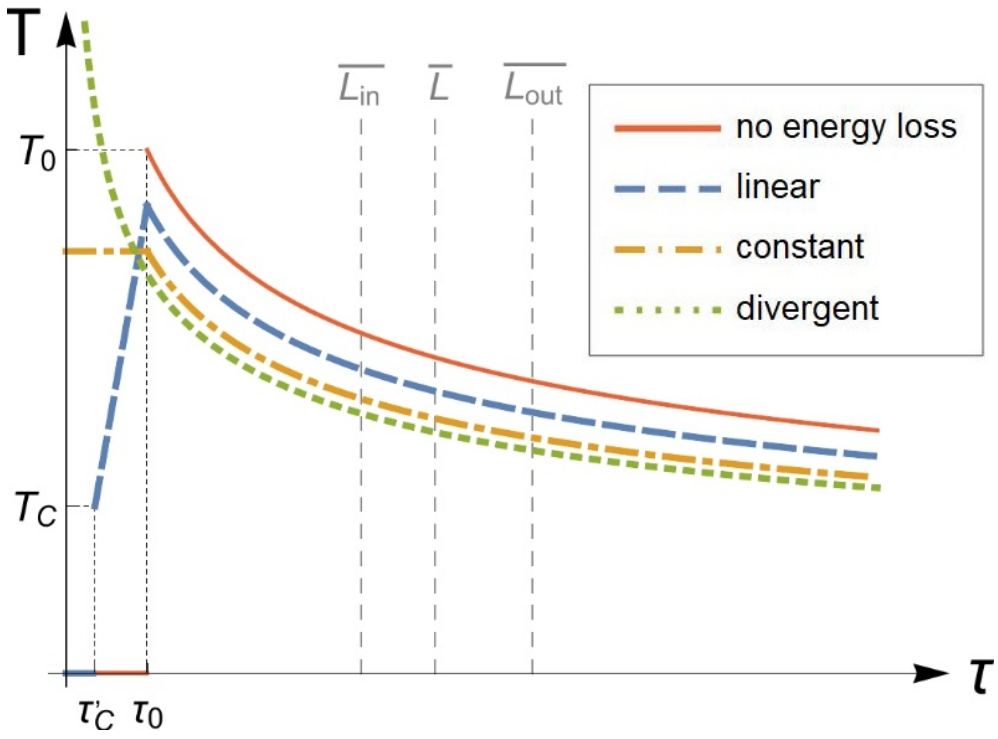

Modified T-profile cases differ not only at initial stages, but represent different evolutions altogether!

D. Zigic, B. Ilic, M. Djordjevic and M. Djordjevic, Phys. Rev. C 101, 064909 (2020)

Sensitivity of high-$p_\perp$ v_2 to modified T profiles

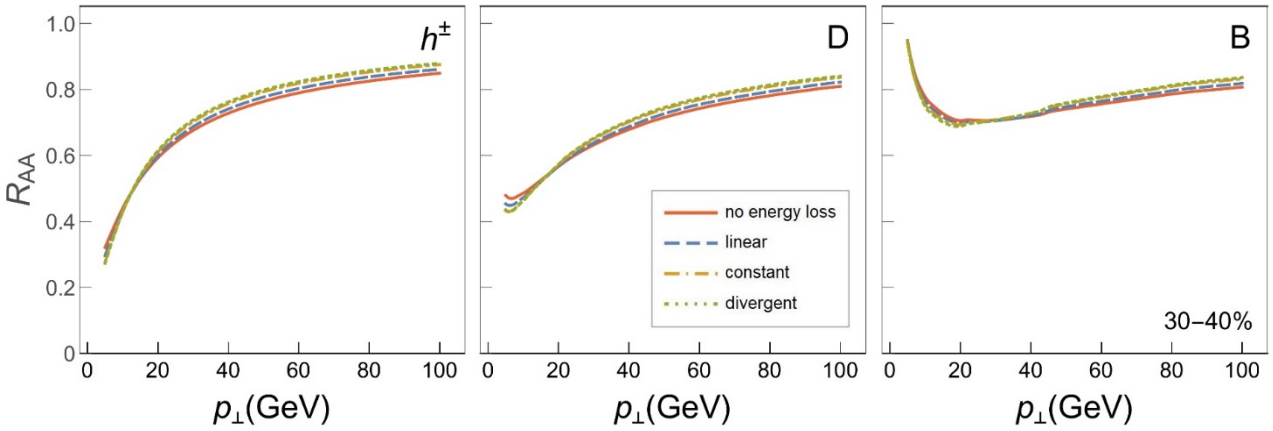

The overlap of high-$p_\perp$ R_{AA} curves in all four modified cases is verified.

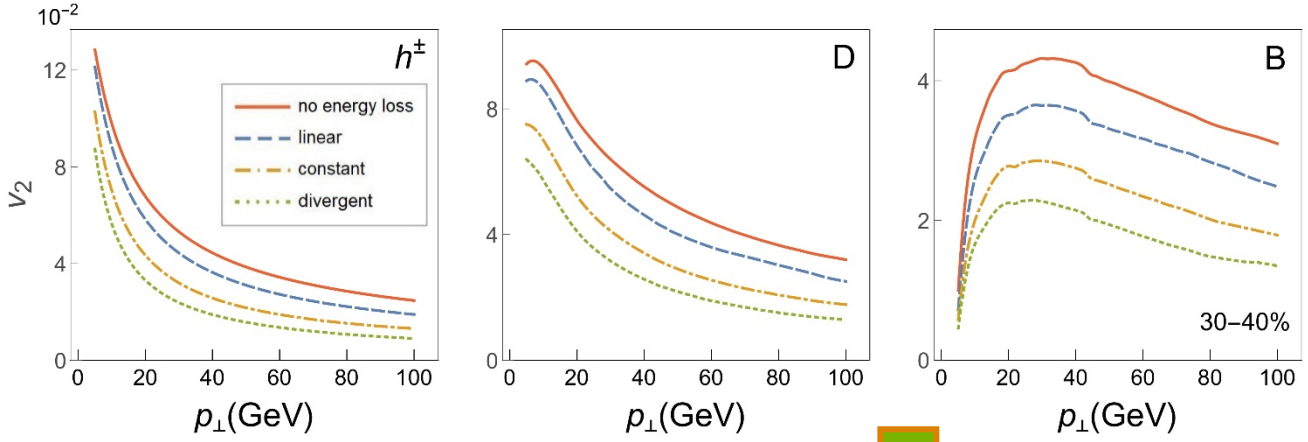

High-$p_\perp$ v_2 is very sensitive to different evolutions.

The highest v_2 is observed in no energy loss case.

D. Zigic, B. Ilic, M. Djordjevic and M. Djordjevic, Phys. Rev. C 101, 064909 (2020)

Sensitivity of high-$p_\perp$ v_2 to modified T profiles

v_2 is very sensitive to these different evolutions.

Why is v_2 affected by these modified T-profile cases?

Are the initial stages at the origin of these v_2 discrepancies?

D. Zigic, B. Ilic, M. Djordjevic and M. Djordjevic, Phys. Rev. C 101, 064909 (2020)

Why is high-$p_\perp$ v_2 affected by modified T profiles?

J. Xu, A. Buzzatti, and M. Gyulassy, JHEP 1408, 063 (2014)

$$v_2 \approx \frac{1}{2}\frac{R_{AA}^{in} - R_{AA}^{out}}{R_{AA}^{in} + R_{AA}^{out}}$$

+ **R_{AA} practically unchanged.**

$$\Rightarrow \quad v_2 \sim R_{AA}^{in} - R_{AA}^{out}$$

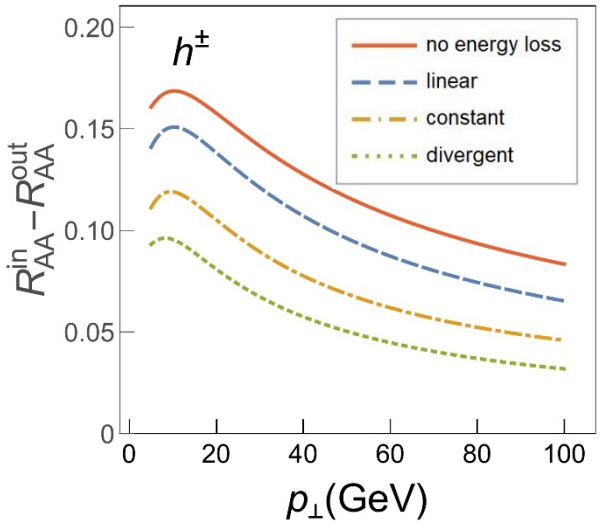

The same curve ordering as for high-$p_\perp$ v_2.

$R_{AA}^{in} - R_{AA}^{out}$ differences are responsible for high-$p_\perp$ v_2 discrepancies.

D. Zigic, B. Ilic, M. Djordjevic and M. Djordjevic, Phys. Rev. C 101, 064909 (2020)

Is PE responsible for high-$p_\perp$ v_2 discrepancies?

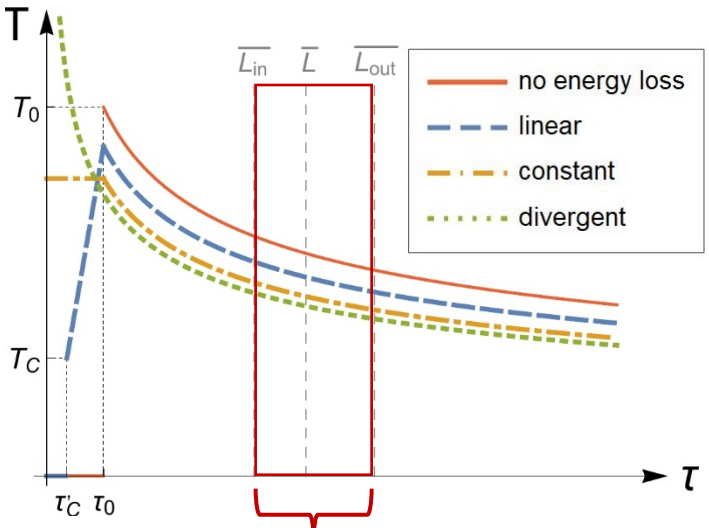

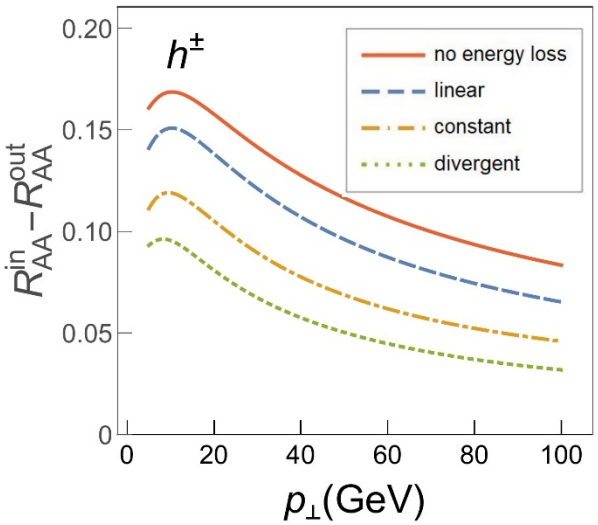

This region contributes to $R_{AA}^{in} - R_{AA}^{out}$ differences.

Large v_2 sensitivity originates from interactions of high-$p_\perp$ parton with *thermalized* QGP, and *not the initial stages*!

D. Zigic, B. Ilic, M. Djordjevic and M. Djordjevic, Phys. Rev. C 101, 064909 (2020)

Fitting energy loss parameters to high-$p_\perp$ R_{AA} experimental data

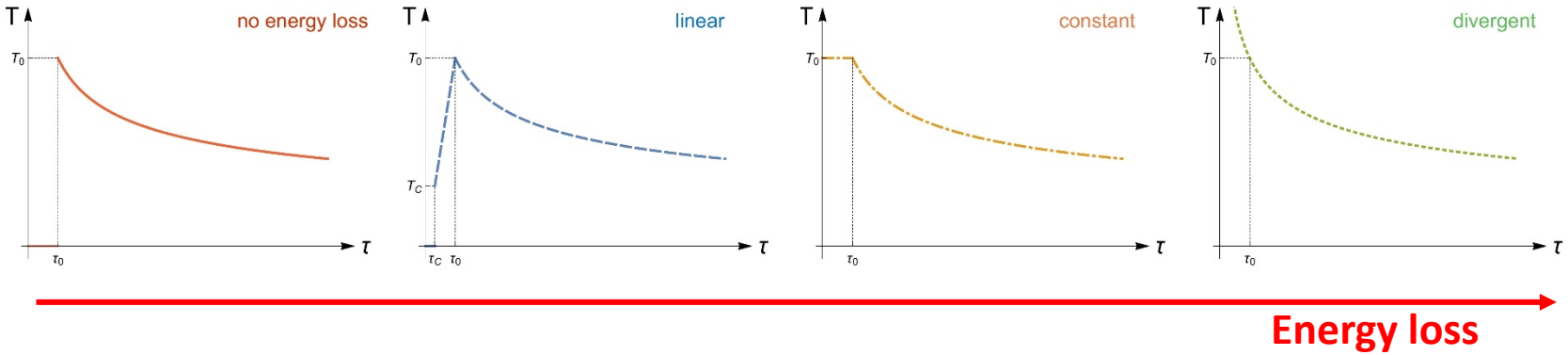

JHEP 1408, 090 (2014), PRL 116, 252301 (2016), PLB 803, 135318 (2020), PRC 96, 064903 (2017), PRC 95, 044901 (2017), PRC 96, 024909 (2017)

Fitting the energy loss (multiplicative fitting factor), to reproduce the high-$p_\perp$ R_{AA} data, individually for different initial stages

An additional fitting factor $C_i^{fit}(p_\perp)$ is introduced in our full-fledged calculations.

Best fits to $R_{AA,nel}$ yield:

T profile case		C_i^{fit}
No E-loss case	(a)	1
Linear case (b)		0.87
Constant case (c)		0.74
Divergent case (d)		0.67

TABLE I: Fitting factors values

Sensitivity of fitted high-$p_\perp$ R_{AA} to IS

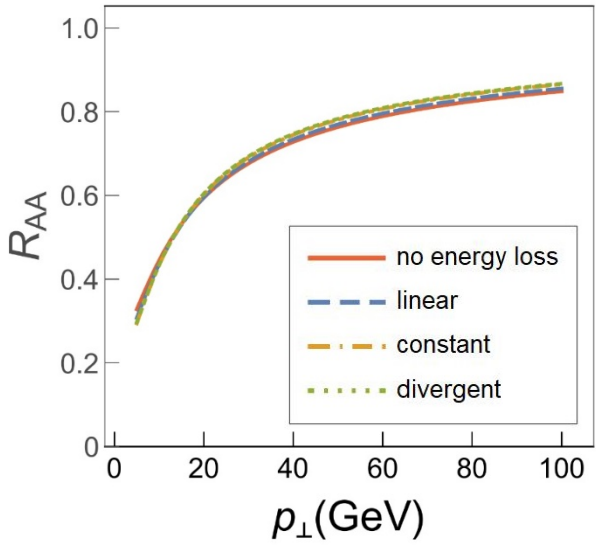

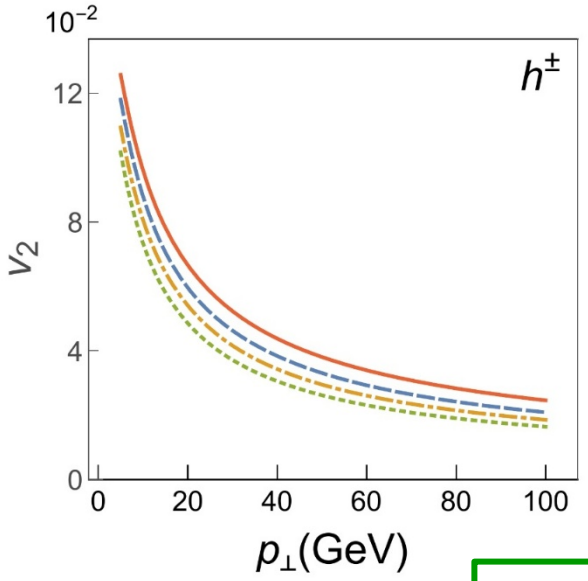

High-$p_\perp$ v_2 is notably affected!

Is this a consequence of early stages?

C. Andres, N. Armesto, H. Niemi, R. Paatelainen and C. A. Salgado, PLB 803, 135318 (2020)

High-$p_\perp$ R_{AA}s are overlapping.

Inconsistent with our previous analysis and also intuitive expectations that higher energy loss at PE leads to lower R_{AA}!

Asymptotic scaling behavior

- **For quantitative explanation of the obtained results**
- **Assumptions:**
  - **Highly energetic jets**
  - **More peripheral collisions**

$$R_{AA} \approx 1 - \xi \overline{T}^{m} \overline{L}^{n}$$

$m \approx 1.2$

$n \approx 1.4$

S. Stojku, B. Ilic, M. Djordjevic, M. Djordjevic arXiv:2007.07851

M. Djordjevic, D. Zigic, M. Djordjevic, J. Auvinen, PRC 99, 061902 (2019)

PLB 791, 236 (2019), JPG 46, 085101 (2019)

$i = lin, const, div$

$$R_{AA,i}^{fit} \approx 1 - C_i(p_\perp) \xi \overline{T}_i^{m} \overline{L}_i^{n}$$

$$R_{AA,i}^{fit} = R_{AA,nel}$$

$$v_{2,i}^{fit} = C_i \gamma_i v_{2,nel}$$

$C_i, \gamma_i < 1$

γ_i approaches 1 at very high $p_\perp$

Differences of fitted $v_{2,i}$ compared to the *nel* case is predominantly a consequence of a decrease in the artificially imposed fitting factor.

Fitting energy loss to individual IS may result in misinterpreting the underlying physics!

PLB 803, 135318 (2020)

J. Xu, A. Buzzatti, and M. Gyulassy, JHEP 1408, 063 (2014)
P. Christiansen, K. Tywoniuk and V. Vislavicius, PRC 89, 034912 (2014)

$$\begin{cases} R_{AA}^{\text{in}}(p_T) \approx \dfrac{\frac{dN_h^{AA}}{dydp_T}(1+2v_2+2v_4\cdots)}{N_{\text{binary}}\frac{dN_h^{pp}}{dydp_T}} = R_{AA}^{h}(1+2v_2+2v_4\cdots) \\ R_{AA}^{\text{out}}(p_T) = \dfrac{\frac{dN_h^{AA}}{dydp_T}(1-2v_2-2v_4\cdots)}{N_{\text{binary}}\frac{dN_h^{pp}}{dydp_T}} = R_{AA}^{h}(1-2v_2-2v_4\cdots) \end{cases}$$

$$v_2 \approx \frac{1}{2}\frac{R_{AA}^{in} - R_{AA}^{out}}{R_{AA}^{in} + R_{AA}^{out}}$$

$$\frac{\mathrm{d}N}{\mathrm{d}\varphi} \propto 1 + 2\sum_{n=1}^{+\infty} v_n \cos\left[n(\varphi - \Psi_n)\right]$$

EbyE effect on v_2

J. Noronha-Hostler, B. Betz, J. Noronha, and M. Gyulassy, PRL 116, 252301 (2016);
S. Shi, J. Liao, and M. Gyulassy, CPC 42, 104104 (2018); 43, 044101 (2019)
S. Cao, L. G. Pang, T. Luo, Y. He, G. Y. Qin, and X. N. Wang, NPPP 289–290, 217 (2017)

$$\Delta E/E \approx \chi \overline{T}^m \overline{L}^n,$$
$$R_{AA} \approx 1 - \frac{l-2}{2}\frac{\Delta E}{E} = 1 - \xi \overline{T}^m \overline{L}^n$$

$$R_{AA,i}^{fit} \approx 1 - C_i \xi \overline{T}_i^m \overline{L}_i^n \approx 1 - C_i(1 - R_{AA,i})$$

$$C_i \approx \frac{1 - R_{AA,i}^{fit}}{1 - R_{AA,i}}$$

$$C_i \approx \frac{v_{2,i}^{fit}}{\gamma_{ia} v_{2,a}}$$

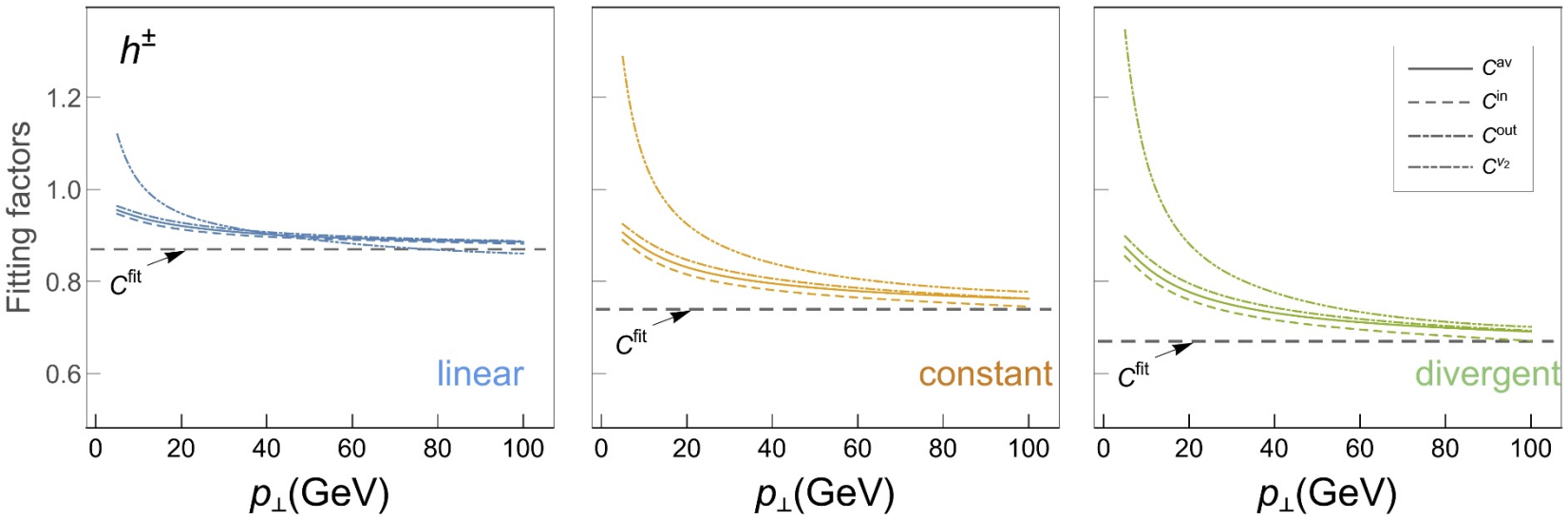

$$C_i^{in} = \frac{1 - R_{AA,i}^{in,fit}}{1 - R_{AA,i}^{in}}, \quad C_i^{out} = \frac{1 - R_{AA,i}^{out,fit}}{1 - R_{AA,i}^{out}},$$

$$C_i^{av} = \frac{1 - R_{AA,i}^{fit}}{1 - R_{AA,i}}, \quad C_i^{v_2} = \frac{1}{\gamma_i} \frac{v_{2,i}^{fit}}{v_{2,a}},$$

Is IS responsible for high-$p_\perp$ v_2 discrepancies?

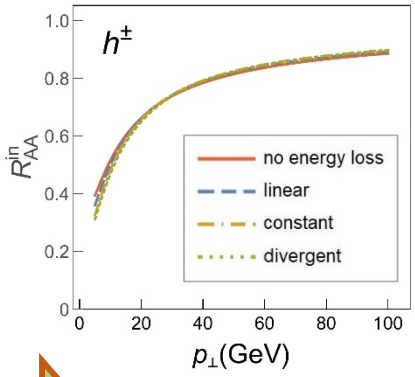

No effect on R_{AA}^{in}.

Only R_{AA}^{out} differences are responsible for v_2 discrepancies.

$-R_{AA} \sim \overline{T}$

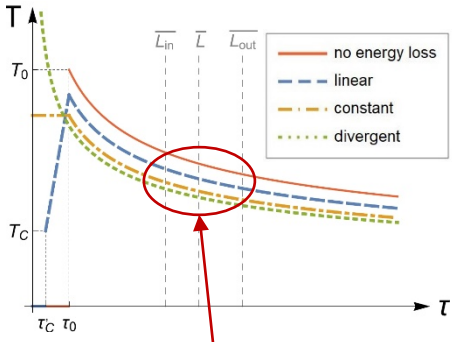

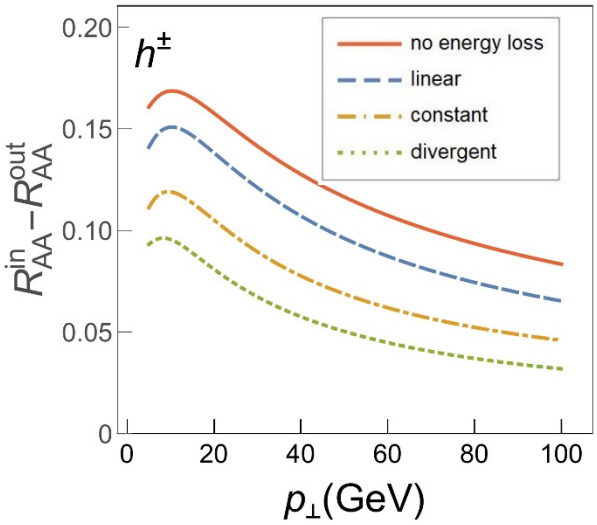

The same curve ordering as modified T profiles in $(\overline{L}_{in}, \overline{L}_{out})$ region.

Only this region contributes to R_{AA}^{out} differences.

v_2 differences originate from interactions of high-$p_\perp$ parton with *thermalized* QGP, and *not the initial stages*!

(T_{eff}) of 304 MeV for 0-40% centrality 2.76 TeV Pb+Pb

ALICE: NPA 904-905 573c (2013).

average medium temperature of 348 MeV in most central 5.02 TeV Pb+Pb

$T_C \approx 150\ MeV$

M. Djordjevic, M. Gyulassy, R. Vogt and S. Wicks, PLB 632, 81 (2006).

$$T_0 \sim (dN_{ch}/dy/A_\perp)^{1/3}$$

$T_0 = 500$ MeV

in most central 5.02 TeV

Pb+Pb

For each centrality region.

$$\frac{dN_{rad}}{dxd\tau}=\frac{C_2(G)C_R}{\pi}\frac{1}{x}\int\frac{d^2\boldsymbol{q}}{\pi}\frac{d^2\boldsymbol{k}}{\pi}\frac{\mu_E^2(T)-\mu_M^2(T)}{[\boldsymbol{q}^2+\mu_E^2(T)][\boldsymbol{q}^2+\mu_M^2(T)]}T\alpha_s(ET)\alpha_s\left(\frac{\boldsymbol{k}^2+\chi(T)}{x}\right)$$

$$\times\left(1-\cos\left(\frac{(\boldsymbol{k}+\boldsymbol{q})^2+\chi(T)}{xE^+}\tau\right)\right)\frac{2(\boldsymbol{k}+\boldsymbol{q})}{(\boldsymbol{k}+\boldsymbol{q})^2+\chi(T)}\left(\frac{\boldsymbol{k}+\boldsymbol{q}}{(\boldsymbol{k}+\boldsymbol{q})^2+\chi(T)}-\frac{\boldsymbol{k}}{\boldsymbol{k}^2+\chi(T)}\right)$$

$$\chi=m_g^2(T)+\mathrm{M}^2x^2$$

M.Djordjevic and M. Gyulassy, PRC 68, 034914 (2003).

$$m_g=\frac{\mu_E}{\sqrt{2}}$$

$$\frac{dE_{coll}}{d\tau}=\frac{2C_R}{\pi\nu^2}\alpha_s(ET)\alpha_s(\mu_E^2(T))\int_0^\infty n_{eq}(|\vec{\boldsymbol{k}}|,T)d|\vec{\boldsymbol{k}}|\left(\int_0^{|\vec{\boldsymbol{k}}|/(1+\nu)}d|\vec{\boldsymbol{q}}|\int_{-\nu|\vec{\boldsymbol{q}}|}^{\nu|\vec{\boldsymbol{q}}|}\omega d\omega+\int_{|\vec{\boldsymbol{k}}|/(1+\nu)}^{|\vec{\boldsymbol{q}}|_{\max}}d|\vec{\boldsymbol{q}}|\int_{|\vec{\boldsymbol{q}}|-2|\vec{\boldsymbol{k}}|}^{\nu|\vec{\boldsymbol{q}}|}\omega d\omega\right)$$

$$\times\left(|\Delta_L(q,T)|^2\frac{(2|\vec{\boldsymbol{k}}|+\omega)^2-|\vec{\boldsymbol{q}}|^2}{2}+|\Delta_T(q,T)|^2\frac{(|\vec{\boldsymbol{q}}|^2-\omega^2)((2|\vec{\boldsymbol{k}}|+\omega)^2+|\vec{\boldsymbol{q}}|^2)}{4|\vec{\boldsymbol{q}}|^4}(\nu^2|\vec{\boldsymbol{q}}|^2-\omega^2)\right)$$

$$D^{\mu\nu}(\omega,\vec{\boldsymbol{q}})=-P^{\mu\nu}\Delta_T(\omega,\vec{\boldsymbol{q}})-Q^{\mu\nu}\Delta_L(\omega,\vec{\boldsymbol{q}})$$

D. Zigic, B. Ilic, M. Djordjevic and M. Djordjevic, Phys. Rev. C 101, 064909 (2020)

Multi-gluon fluctuations

M. Gyulassy, P. Levai, I. Vitev, PLB 538,282 (2002)

Poisson distribution:

$$P(k \text{ events in interval}) = \frac{\lambda^k e^{-\lambda}}{k!}$$

where

- λ is the average number of events per interval

Poisson expansion $P(\epsilon, E) = \sum_{n=0}^{\infty} P_n(\epsilon, E)$ $\quad \epsilon = \sum_i \omega_i / E$

$$P_0(\epsilon, E) = e^{-\langle N^g(E)\rangle}\delta(\epsilon)$$

$$P_1(\epsilon, E) = e^{-\langle N^g\rangle}\rho(\epsilon, E)$$

$$\rho(x) = dN_g/dx = \sum_{n=1}^{\infty} \rho^{(n)}(x)$$

$$P_{n+1}(\epsilon, E) = \frac{1}{n+1}\int_{x_0}^{1-x_0} dx_n\, \rho(x_n, E) P_n(\epsilon - x_n, E)$$

$$= \frac{e^{-\langle N^g(E)\rangle}}{(n+1)!}\int dx_1 \cdots dx_n\, \rho(x_1, E)\cdots\rho(x_n, E)\rho(\epsilon - x_1 - \cdots - x_n, E)$$

$$\int_0^{\infty} d\epsilon\, P(\epsilon, E)\epsilon = \frac{\Delta E}{E}$$

$$m_g = m_\infty = \sqrt{\Pi_T(p_0/|\vec{\mathrm{p}}| = 1)} = \mu_E/\sqrt{2}$$

Effective gluon mass

M. Djordjevic and M. Gyulassy, PRC 68:034914 (2003)